Synthetic Metals 160 (2010) 561–565

Contents lists available at ScienceDirect

Synthetic Metals

journal homepage: www.elsevier.com/locate/synmet

Porous carbon nanotube electrodes supported by natural polymeric membranes for PEMFC

Young Soo Yun, Hyeonseong Bak, Hyoung-Joon Jin*

Department of Polymer Science and Engineering, Inha University, 253 Yonghyun-Dong, Nam-Gu, Incheon 402-751, Republic of Korea

ARTICLE INFO

Article history:
Received 18 September 2009
Received in revised form 2 December 2009
Accepted 5 December 2009
Available online 8 January 2010

Keywords:
Multiwalled carbon nanotube
Proton exchange membrane fuel cells
Electrode
Porous carbon

ABSTRACT

A new type of porous multiwalled carbon nanotube (MWCNT) electrode with a macroporous networking inner-structure was prepared. First, the MWCNTs were homogeneously introduced inside and outside of a bacterial cellulose membrane with a 3D inter-connected network structure using ultrasound treatment and vacuum filtration in order to form the GDL. Second, the CL was formed on the surface of the GDL through vacuum filtration of the Pt incorporated MWCNTs (Pt/MWCNTs). Finally, the electrode was created through freeze-drying. The final electrode had a sheet resistance of 80 Ω/□ and an electro-chemical active surface area (ECSA) of 10.1 m^2/g. Although the ECSA of the electrode did not have the efficiency (14.3 m^2/g) of a typical electrode (carbon cloth/Pt/carbon black), these results suggested that the new type of electrode has potential as a proton exchange membrane fuel cell.

1. Introduction

The changing climate and the decreasing availability of fossil fuels are creating energy concerns and leading to the development of alternative power sources. Proton exchange membrane fuel cells (PEMFC) that utilize hydrogen as fuel have gained attention because of their energy efficiency, which is higher than that of combustion engines, and low pollutant emissions. Additionally, the potential of PEMFCs is high because hydrogen can be generated from a variety of sources. However, a wide application of these cells is hindered by their high cost. One important goal in PEMFC technology is reducing the amount of electro-catalyst required without sacrificing the performance. Therefore, the utilization of Pt catalysts plays an important role in the practical application of PEMFCs. Many studies have focused on the efficient utilization of Pt catalysts [1–4]. Catalyst support technology is an effective approach that lowers the amount of catalyst needed and, meanwhile, improves the catalytic activity of the supported catalysts. The catalytic activity of the Pt based catalysts strongly depends on the catalyst support, which determines the size and degree of dispersion of the catalysts as well as the distribution and stabilization of the catalyst particles [5]. Normally, carbon black Vulcan XC-72 (VC) is widely used as an electro-catalyst support [6]. However, carbon black contains a large number of micropores [7,8], which are sometimes too small for the electrolyte polymer, resulting in entrapped Pt nanoparticles that do not contribute to the electrode reactions. Carbon nanotubes (CNTs) are attractive materials for catalyst support in PEMFC because of their morphology and interesting properties such as nanometer size, highly accessible surface area, corrosion resistance, good electrical conductivity, and high stability [2,3,9]. In previous studies, CNTs have been used as the support material for Pt catalyst nanoparticles in order to achieve higher PEMFC and direct methanol fuel cell (DMFC) performances [10–12].

The electrodes of PEMFCs consist of a gas diffusion layer (GDL) and a catalyst layer (CL). First, the reaction gases successfully diffuse into the catalyst layer and uniformly spread thereon because of the porous structure of the GDL. Second, the electrons that are generated through the catalysis are drained from the electrode and enter the external circuit. Therefore, the GDL must be a porous material and a good electrical conductor [13].

Bacterial cellulose (BC) is a sustainable natural polymer that belongs to the polysaccharide family and is produced by acetic bacteria, e.g. *Acetobacter xylinum*. BC has a unique structure and properties compared to other types of cellulose in terms of its purity, high crystallinity, and high mechanical strength [14–16]. Above all, BC membranes have macroporous 3D-inter-connected network structures [17].

In this study, porous CNT electrodes with a macroporous networking inner-structure were prepared and functioned both as the GDL and CL. A bacterial cellulose membrane (BCM) was used to support the macroprous CNT network. In this process, the multiwalled carbon nanotubes (MWCNTs) were homogeneously introduced to the inside and outside of the BCM using ultrasound treatment and vacuum filtration without any damage to the macroporous 3D-network structure. Then, the Pt incorporated MWCNTs (Pt/MWCNTs) were introduced onto the surface

* Corresponding author. Tel.: +82 32 860 7483.
E-mail address: hjjin@inha.ac.kr (H.-J. Jin).

0379-6779/$ – see front matter © 2009 Elsevier B.V. All rights reserved.
doi:10.1016/j.synthmet.2009.12.003

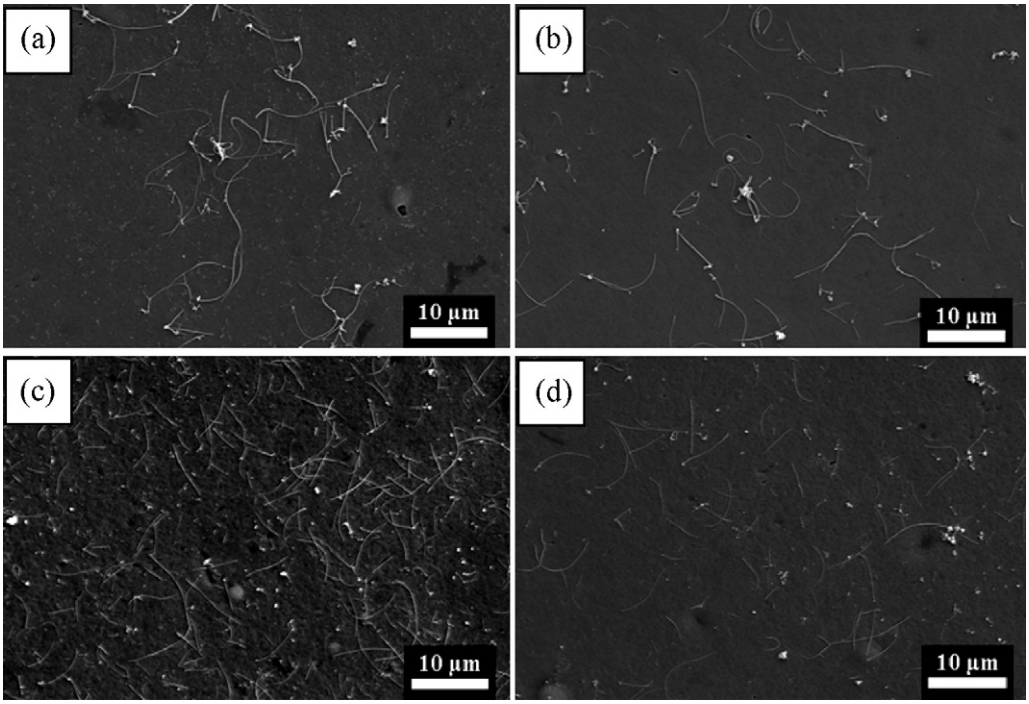

Fig. 1. SEM images of (a) the pristine MWCNTs and the MWCNTs that were acid treated for (b) 6, (c) 18, and (d) 24 h.

Table 1
Sheet Resistance and aspect ratio of the acid treated MWCNTs.

Sample name	Sheet resistance (Ω/□)	Aspect ratio
Pristine MWCNTs	2.0×10^{0}	218
Acid treated MWCNTs for 6 h	1.6×10^{0}	144
Acid treated MWCNTs for 12 h	1.3×10^{0}	143
Acid treated MWCNTs for 18 h	7.6×10^{-1}	127
Acid treated MWCNTs for 24 h	7.8×10^{-1}	86
Acid treated MWCNTs for 48 h	7.0×10^{-1}	79

of the MWCNT incorporated BCM through an easy vacuum filtration method. This electrode, based on the MWCNTs and the BCM, was created through freeze-drying. The morphological, electrical, and electro-chemical properties of the electrode were investigated.

2. Experimental details

2.1. Preparation of BCM

Gluconacetobacter xylinum BRC-5 was cultured on a Hestrin and Schramm (HS) medium, which was composed of 2% (w/v) glucose, 0.5% (w/v) yeast extract, 0.5% (w/v) bacto-peptone, 0.27% (w/v) disodium phosphate, and 0.115% (w/v) citric acid. The cells were precultured in a test tube for seven days and then were inoculated into a 60 mm × 15 mm Petri dish containing 10 mL of the HS medium. The cells in the Petri dish were statically incubated at 30 °C for seven days. The BCMs were purified in a 0.25 M NaOH solution for 48 h at room temperature in order to eliminate the cells and components of the culture liquid. Then the pH of the BCM was lowered to 7.0 through repeated washing with distilled water. The purified BCMs were stored in distilled water at 4 °C to prevent drying.

2.2. Chemical treatment of MWCNTs

The as-received MWCNTs (NCT, Japan) were treated with acid using the following procedure that was reported in an earlier study [18]. The MWCNTs were treated in an acid mixture (sulfuric acid/nitric acid = 3:1 (v/v)) at 60 °C for various amounts of time (6, 12, 18, 24, and 48 h). Any impurities within the MWCNTs were removed through the acid treatment and carboxylic and hydroxyl functional groups were introduced onto the surface of the MWCNTs.

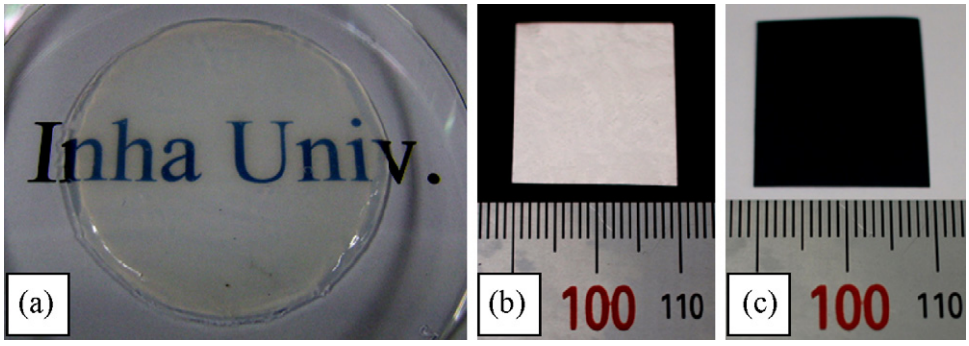

Fig. 2. Photo images of (a) the pristine BCM, (b) the freeze-dried BCM, and (c) the MWCNT incorporated BCM electrode.

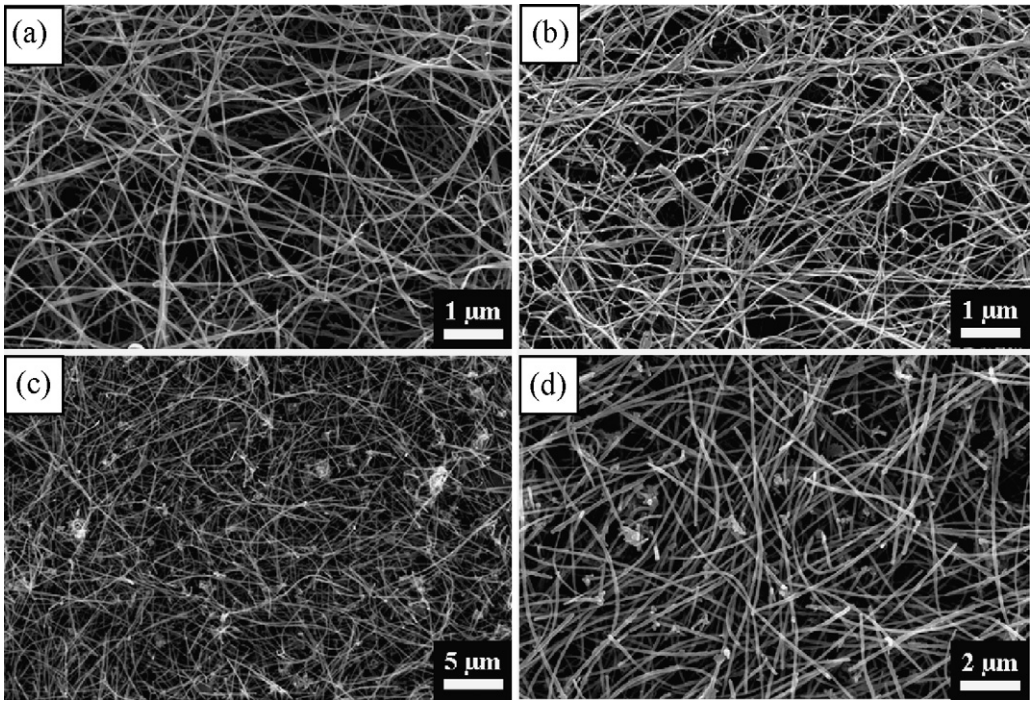

Fig. 3. SEM images of (a) the freeze-dried BCM in water, (b) the freeze-dried BCM in tert-butanol, and (c), (d) the MWCNT incorporated BCM electrode.

2.3. Synthesis of MWCNT supported Pt catalysts

The MWCNT supported Pt nanoparticle catalysts were prepared using the modified microwave-assisted polyol process described by Liu et al. [19] Specifically, 5.0 mL of an aqueous solution of 0.05 M $H_2PtCl_6{\cdot}6H_2O$ was mixed with 150 mL of ethylene glycol in a 250 mL beaker. Then 1.75 mL of 0.4 M KOH was added dropwise to the vigorously stirred solution to adjust the pH to around 8–9. Next, the required amount of acid treated MWCNTs (a-MWCNTs) was added to the mixture and ultrasonicated for 30 min. Then the beaker containing the mixture of Pt salt and the a-MWCNTs was heated in a household microwave oven (SAMSUNG RE-C20DV, 2450 MHz, 700 W) for 100 s, and the resulting suspension was vigorously stirred overnight and filtered. The residue (mainly a-MWCNT-supported Pt catalyst) was thoroughly washed using deionized water and dried at 353 K overnight.

2.4. Preparation of porous MWCNT electrode supported by BCM

The a-MWCNTs were dispersed in distilled water using ultrasound treatment. The BCM was immersed in the aqueous a-MWCNT dispersion, and ultrasound treatment was applied for three hours. In this process, the a-MWCNTs penetrated into the inner and outer network structures of the BCM and were also introduced onto the surface of the a-MWCNT incorporated BCM through an easy vacuum filtration method. Using the same method, the Pt/MWCNTs were introduced onto the

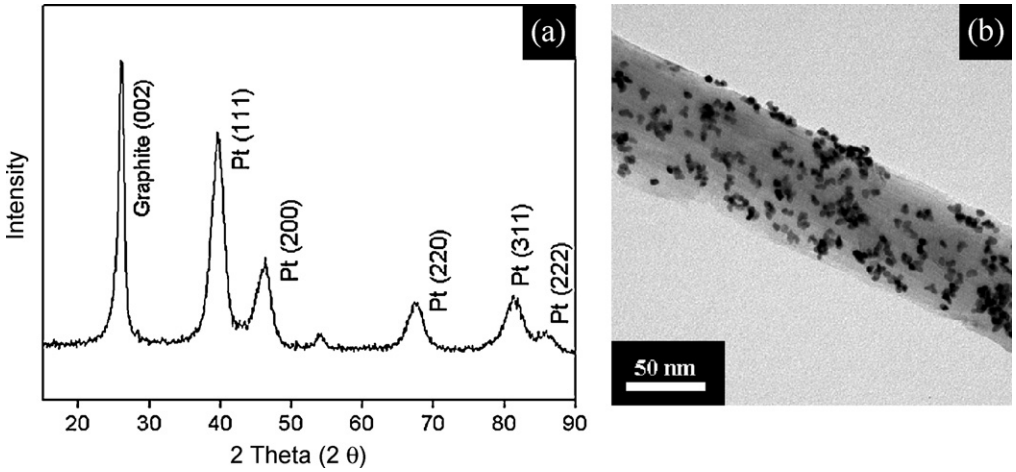

Fig. 4. (a) X-ray diffraction pattern of the 20 wt.% Pt/MWCNT catalyst. The mean Pt particle size of 4.8 nm was estimated from the Pt (2 2 0) peak. (b) TEM image of the 20 wt.% Pt/MWNT catalyst. The 4–5 nm Pt particles were reasonably distributed on the surface of the MWCNT.

other side of the a-MWCNT incorporated BCM. The BMC was immersed in tert-butanol for several days and freeze-dried for 48 h in order to dry it without damaging the macroporous 3D-network.

2.5. Characterization

The morphologies of the MWCNTs and MWCNT incorporated BCM were observed using field emission scanning electron microscopy (FESEM, S-4300SE, Hitachi, Japan) at an accelerating voltage of 15 kV after the samples were pre-coated with a homogeneous Pt layer through ion sputtering (E-1030, Hitachi, Japan). The aspect ratios of the MWCNTs were calculated by measuring the diameter and length of each MWCNT from several FESEM images and then were statistically computed using a software program. The electrical conductivities of the MWCNT and the porous MWCNT electrode were measured using a four-probe method with an electrical conductivity meter (Hiresta-UP MCP-HT450, Mitsubishi Chemical, Japan). The X-ray diffraction (XRD) measurements for the electrode and the supported Pt catalysts were carried out using a Rigaku DMAX 2500 with Cu Kα radiation (wavelength λ = 0.154 nm) at 40 kV and 100 mA. The catalysts were examined using transmission electron microscopy (TEM, CM200, Philips, USA). The amount of MWCNTs that were introduced into the BC membrane was calculated using thermogravimetric analysis (TGA, Q50, TA instruments, UK) from 20 to 800 °C at a heating rate of 10 °C/min under a nitrogen atmosphere.

The electro-chemical active surface area (ECSA) of Pt in the carbon-supported Pt catalysts was estimated using a three-electrode electro-chemical cell, and the cyclic voltammetric (CV) measurements were conducted in 0.5 M H_2SO_4 at room temperature with a scan rate of 50 mV/s from −0.2 V to 1.2 V. In all the measurements, Pt gauze and Ag/AgCl were used as the counter and reference electrodes, respectively. A typical electrode was prepared by simply spraying 20 wt.% Pt/carbon black catalysts (Johnson Matthey) onto a carbon cloth. The ECSA of the typical electrode was compared to the porous MWCNT electrode. All of the electrodes had platinum loading of 0.4 mg/cm^2.

3. Results and discussion

The morphologies of the MWCNTs are shown in Fig. 1. The pristine MWCNTs had a large aspect ratio and were aggregated with each other. The MWCNTs became more chopped and dispersed in the substrate as the acid treatment time increased. Overall, the a-MWCNTs were over several micrometers long and had rod-like straight morphologies rather than winding morphologies. The physical properties of the MWCNTs depended on the degree of bent curvature of the MWCNT [20]. The straight morphologies of the a-MWCNTs contributed to the increased electrical conductivity. Additionally, the chemical doping the carbon nanotubes with an oxidizing agent significantly enhanced the conductivity [21,22]. Table 1 shows the sheet resistance and aspect ratio of the a-MWCNTs. The sheet resistance and aspect ratio independently decreased as the treatment time increased. Therefore, the appropriate acid treatment time for MWCNTs was examined in order to achieve a low sheet resistance and a large aspect ratio. The MWCNTs that were treated for 18 h in an acid mixture (sulfuric acid/nitric acid = 3:1 (v/v)) at 60 °C) had a relatively low sheet resistance and a large aspect ratio.

Fig. 2 shows photo images of the pristine BCM, freeze-dried BCM, and MWCNT incorporated BCM electrode. The pristine BCM was visibly transparent and jelly-like, and exhibited both a high toughness and flexibility (Fig. 2(a)). The freeze-dried BCM was opaque and monolithic (Fig. 2(b)). The MWCNT incorporated BCM

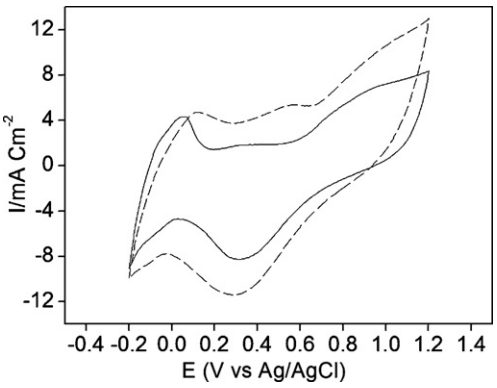

Fig. 5. Cyclic voltammograms of the porous MWCNT electrode (dotted line) and the typical electrode (carbon cloth/Pt/carbon black) (solid line) in 0.5M H_2SO_4 with a scan rate of 50 mV/s. The catalyst loading in the working electrode was 0.4mg Pt/cm^2.".

electrode exhibited a homogeneous black color and a monolithic structure. The freeze-drying method was safe and economical because the pore liquid was frozen and then sublimed under a vacuum. Additionally, solvent exchange was not necessary if the wet gel was prepared in an aqueous solution. Despite these advantages, the porous structures of the cryogels tended to be destroyed as the ice crystallized. Therefore, the solvent that the pristine BCM was exchanged with tert-butanol in order to dry the membrane without damage to the macroporous 3D-network structure. The microscopic morphologies of the freeze-dried BCM and the MWCNT incorporated BCM electrode were investigated using SEM (Fig. 3). The nano-sized fibrils of the pristine BC were three dimensionally inter-connected, and this structure resulted in a large number of macropores (Fig. 3(a)). After the solvent of the BCM was exchanged with tert-butanol, the macroporous 3D-network structure was not damaged except some shrinkage (Fig. 3(b)). Fig. 3(c) and (d) shows the surface morphologies of the BCM electrode containing MWCNTs. The macroporous MWCNT layers were formed on the inner and outer BC membrane through ultrasound treatment and vacuum filtration. Although no surfactant or chemical reagent was used, the MWCNTs were firmly attached to the BCM. Even after ultrasound treatment in distilled water for several minutes, no discernible black particles were observed in the solution, suggesting a strong adhesion between the MWCNTs and the BC membrane as well as a strong physical interaction between the MWCNTs.

The XRD pattern of the Pt/CNT sample is shown in Fig. 4(a). The diffraction peak observed at 23–27° was attributed to the hexagonal graphite structure (0 0 2), and showed that CNTs had a good electric conductivity. The mean particle size of the Pt nanoparticles was estimated from the isolated Pt (2 2 0) peak with the Scherrer equation [23]. The mean particle size was approximately 4.8 nm, which was consistent with the typical TEM images of the Pt/MWCNT samples (Fig. 4(b)). The 20 wt.% Pt nanoparticles were loaded onto the surface of MWCNTs and reasonably distributed. These Pt/MWCNTs were introduced onto the surface of the a-MWCNT incorporated BCM using vacuum filtration (2 mg/cm^2 Pt/MWCNTs). The sheet resistance of the a-MWCNT incorporated BCM with 40 wt.% MWCNTs was 230 Ω/□. The sheet resistance of the Pt/MWCNTs incorporated BCM was 80 Ω/□. Although the sheet resistance of Pt/MWCNTs incorporated BCM electrode was higher than the a-MWCNTs, the electrode had a high enough for electro-chemical devices. Fig. 5 shows the cyclic voltammogram for the hydrogen adsorption on the Pt/MWCNT incorporated BCM electrode and the typick electrode at a scan rate of 50 mV/s over a potential range of −0.2–1.2 V. The characteris-

tic peaks in the negative region (−0.2–0 V) were attributed to the atomic hydrogen adsorption on the Pt surface and reflected the ECSA of Pt [24].

$$\text{ECSA}\,[\text{cm}^2/\text{g of Pt}] = \frac{\text{Charge}\,[Q_H, \mu\text{C/cm}^2]}{210\,[\mu\text{C/cm}^2] \times \text{electrode loading}\,[\text{g of Pt/cm}^2]} \quad (1)$$

The ECSAs were calculated using Eq. (1) and the integration of the voltammograms in Fig. 5. The typical carbon cloth/Pt/carbon black electrode and Pt/MWCNT incorporated BCM electrode had ECSAs of 14.3 and 10.1 m^2/g of Pt, respectively. The ECSA of the Pt/MWCNT incorporated BCM electrode was not efficient as the typical electrode and direct experimental evidence was not conducted to see the relation between the surface area and the ability of gas diffusion function of the porous MWCNT, however, this electrode might be used as an electrode in PEMFCs.

4. Conclusion

A new type of porous (MWCNT) electrode with macroporous networking inner-structure was prepared, and this electrode functioned both as the GDL and CL. To form the GDL, 40 wt.% a-MWCNTs penetrated into the inner and outer network structure of the BCM and were firmly attached to the BCM without any surfactant or chemical reagent. No discernible black particles were present in the solution even after ultrasound treatment in distilled water for several minutes. Then 20 wt% Pt/MWCNTs were introduced onto the surface of the GDL using vacuum filtration (2 mg/cm^2 Pt/MWCNTs) in order to form the CL. This electrode had a sheet resistance of 80 Ω/□ and an ECSA of 10.1 m^2/g. Although the ECSA of the electrode was not as efficient (14.3 m^2/g) as a typical electrode (carbon cloth/Pt/carbon black), these results suggested that the new type of electrode could be potentially used in PEMFCs.

Acknowledgements

This work was supported by the Korea Science and Engineering Foundation (KOSEF) grant funded by the Korea government (MEST) (R11-2005-065).

References

[1] E. Antolini, Appl. Catal. B: Environ. 88 (2009) 1.
[2] C. Wang, M. Waje, X. Wang, J.M. Tang, R.C. Haddon, Y. Yan, Nano Lett. 4 (2004) 345.
[3] A.L.M. Reddy, S. Ramaprabhu, J. Phys. Chem. C 111 (2007) 16138.
[4] S.J. Yoo, Y.-H. Cho, H.-S. Park, J.K. Lee, Y.-E. Sung, J. Power Sources 178 (2008) 547.
[5] B. Fang, J.H. Kim, M. Kim, J.-S. Yu, Chem. Mater. 21 (2009) 789.
[6] A.S. Arico, L. Pino, P.L. Antonucci, N. Giordano, Carbon 28 (1990) 599.
[7] K.-W. Park, B.-K. Kwon, J.-H. Choi, I.-S. Park, Y.-M. Kim, Y.-E. Sung, J. Power Sources 109 (2002) 439.
[8] M. Uchida, Y. Aoyama, M. Tanabe, N.N.E. Yanagihara, A. Ohta, J. Electrochem. Soc. 142 (1995) 2572.
[9] G. Girishkumar, M. Rettker, R. Underhile, D. Binz, K. Vinodgopal, P. McGinn, P. Kamat, Langmuir 21 (2005) 8487.
[10] W. Li, C. Liang, J. Qiu, W. Zhou, H. Han, Z. Weia, G. Suna, Q. Xina, Carbon 40 (2002) 787.
[11] W. Li, C. Liang, W. Zhou, J. Qiu, Z. Zhou, G. Sun, Q. Xin, J. Phys. Chem. B 107 (2003) 6292.
[12] W. Li, X. Wang, Z. Chen, M. Waje, Y. Yan, Langmuir 21 (2005) 9386.
[13] J.-H. Lin, W.-H. Chen, Y.-J. Su, T.-H. Ko, Energy Fuels 22 (2008) 1200.
[14] J.W. Hwang, Y.K. Yang, J.K. Hwang, Y.R. Pyun, Y.S. Kim, J. Biosci. Bioeng. 88 (1999) 183.
[15] M. Iguchi, S. Yamanaka, A. Budhiono, Mater. Sci. 35 (2000) 261.
[16] D. Klemm, D. Schumann, U. Udhardt, S. Marsch, Prog. Polym. Sci. 26 (2001) 1561.
[17] S.H. Yoon, H.-J. Jin, M.-C. Kook, Y.R. Pyun, Biomacromolecules 7 (2006) 1280.
[18] S.-M. Kwon, H.-S. Kim, H.-J. Jin, Polymer 50 (2009) 2786.
[19] Z. Liu, L.M. Gan, L. Hong, W. Chen, J.Y. Lee, J. Power Sources 139 (2005) 73.
[20] H.S. Lee, C.H. Yun, H.M. Kim, C.J. Lee, J. Phys. Chem. C 111 (2007) 18882.
[21] R. Graupner, J. Abraham, A. Vencelovaĭ, T. Seyller, F. Hennrich, M.M. Kappes, A. Hirsch, L. Ley, Phys. Chem. Chem. Phys. 5 (2003) 5472.
[22] U. Dettlaff-Weglikowska, V. Skaĭkalovaĭ, R. Graupner, S.H. Jhang, B.H. Kim, H.J. Lee, L. Ley, Y.W. Park, S. Berber, D. Tomaĭnek, S. Roth, J. Am. Chem. Soc. 127 (2005) 5125.
[23] B. Seger, P.V. Kamat, J. Phys. Chem. C 113 (2009) 7990.
[24] M. Søgaard, M. Odgaard, E.M. Skou, Solid State Ionics 145 (2001) 31.